

# Modeling the Shape and Evolution of Normal-Fault Facets

Gregory E. Tucker<sup>1\*</sup>, Frog2<sup>1,2</sup>, Frog3<sup>3</sup>

<sup>1</sup>Cooperative Institute for Research in Environmental Sciences and Department of Geological Sciences,  
University of Colorado, Boulder, Colorado, USA.

<sup>2</sup>Frog Pond.

<sup>3</sup>Toad Pond.

## Key Points:

- Evolution of raw ensemble forecast (Replaced: skill replaced with: skills)
- Future benefits from statistical post-processing
- Global distribution of forecast skill development

---

\*Current address, McMurdo Station, Antarctica

Corresponding author: A. B. Smith, email@address.edu

12      **Abstract**

13      this is a highly abstract paper

14      **1 Introduction**

15      Outline for potential short-ish paper on facet morphology:

16      I. Introduction

17      Morphology of normal-fault facets poses some interesting questions: - variations  
18      in facet dip angle (from less than 10 degrees to over 30 degrees) - despite planar mor-  
19      phology, dip angle of facet is almost always less than the dip angle of the fault - some  
20      facets are mantled by a mostly continuous mantle of soil, whereas others are rocky and  
21      host discontinuous, patchy soil - in some cases, the mapped fault trace lies at the base  
22      of the facet, where in others, the fault trace occurs in mid-slope, coinciding with a tran-  
23      sition from rock to colluvium but without a clear break in slope

24      Literature review: facets have intrigued geoscientists both because of their strik-  
25      ing morphology, and because of what they can reveal about tectonic motion and earth-  
26      quake hazards. Various refs: Carole Petit, McCalpin, Tucker et al., 2011, etc., etc.

27      Need a process-based model that can account for the basic morphology of facets,  
28      and the key variations in morphology that are observed.

29      II. Normal-Fault Facets in the Italian Central Apennines and the central western  
30      United States

31      Show photos, lidar images, for facets in Wasatch and north, and in Italy

32      III. Cellular Model of Facet Evolution

33      A. Why a Cellular Model?

34      motivation for using this kind of model, citing Grain Hill paper and noting that  
35      process params can be pinned

36      B. Model Description describe model

37      C. Experimental Design

38 goal is to determine: - what are the necessary and sufficient conditions to repro-  
 39 duce the common morphology of a facet: planar with thin soil cover? - can the model  
 40 account for observed range in facet morphology and soil cover? - what are the key con-  
 41 trols on slope gradient, profile shape, and regolith cover fraction and thickness?

42 **IV. Results**

43 **A. Weathering-limited facets**

44 demonstrate that one recaptures Tucker et al. 2011 behavior when  $d' \ll w'$ : ex-  
 45 periments in which the predicted angle should be 60 degrees (no weathering), 45, 30, 15.

46 **B. Influence of  $d'$  and  $w'$**

47 3x3 (or maybe 5x5) plot in  $d'$  and  $w'$  space

48 plot of facet dip angle in  $d'$  and  $w'$  space (from talk, showing family of curves)

49 **C. (optional) what if rock or soil can dissolve, a la Italian carbonates? (dissolution  
 50 rule)**

51 **D. (optional) baselevel effects** - what happens when either you have a basal stream  
 52 cutting down or a hangingwall valley aggrading? This would require having a modifi-  
 53 cation that would add or remove rock cells along the left edge

54 **E. what sets the effective E vs S relation?** refer back to T et al., 2011, noting re-  
 55 strictive assumption of slope-independent erosion rate

56 **V. Discussion**

57 - model accounts for basic morphology and shape. necessary and sufficient condi-  
 58 tions for planar facet with dip angle less than fault dip: weathering of rock plus distur-  
 59 bance, and [something about limits, i.e., curvature appears when  $d'/w' > ...$ ]

60 - facet angle close to angle of repose is an attractor state, because below that an-  
 61 gle, the transport rate and length scale of produced regolith goes way down

62 - for this reason, it should be common to observe cases where the fault trace cuts  
 63 across a roughly uniform slope, marking a transition from eroding rock to aggrading col-  
 64 luvium

65 - cases that do NOT show this morphology are anomalies, likely reflecting strong  
66 baselevel control apart from simply fault slip (aggradation or incision)

67 - facet dip angle is set by ...

68 - facet soil cover depth and spatial continuity set by ...

69 - facets are predicted to become concave-up when ...

70 - to test these ideas, we need cosmos on facet slopes!

71 VI. Conclusions

72 model accounts for facet morphology as a consequence of tectonic motion, rock weathering  
73 and regolith disturbance

74 variations in facet morphology can be explained as a consequence of ...

75 erosion rate does depend on slope gradient, like thus-and-such

76 need cosmos to test these predictions

77 TENTATIVE LIST OF FIGURES:

78 - pix of facets

79 o bar graph of regolith thickness and percent cover on a bunch of facets

80 - model illustration combining list of states with hexagons, with schematic example  
81 transitions from Grain Hill

82 - T et al 2011 schematic

83 = figure showing model diss-lim runs at varying S', compared with analytical

84 - model vs analytical diss-lim

85 - 4x4 of sim profiles in d' vs w' space

86 - plot of gradient in d' and w' space

87 - same for reg cover proportion

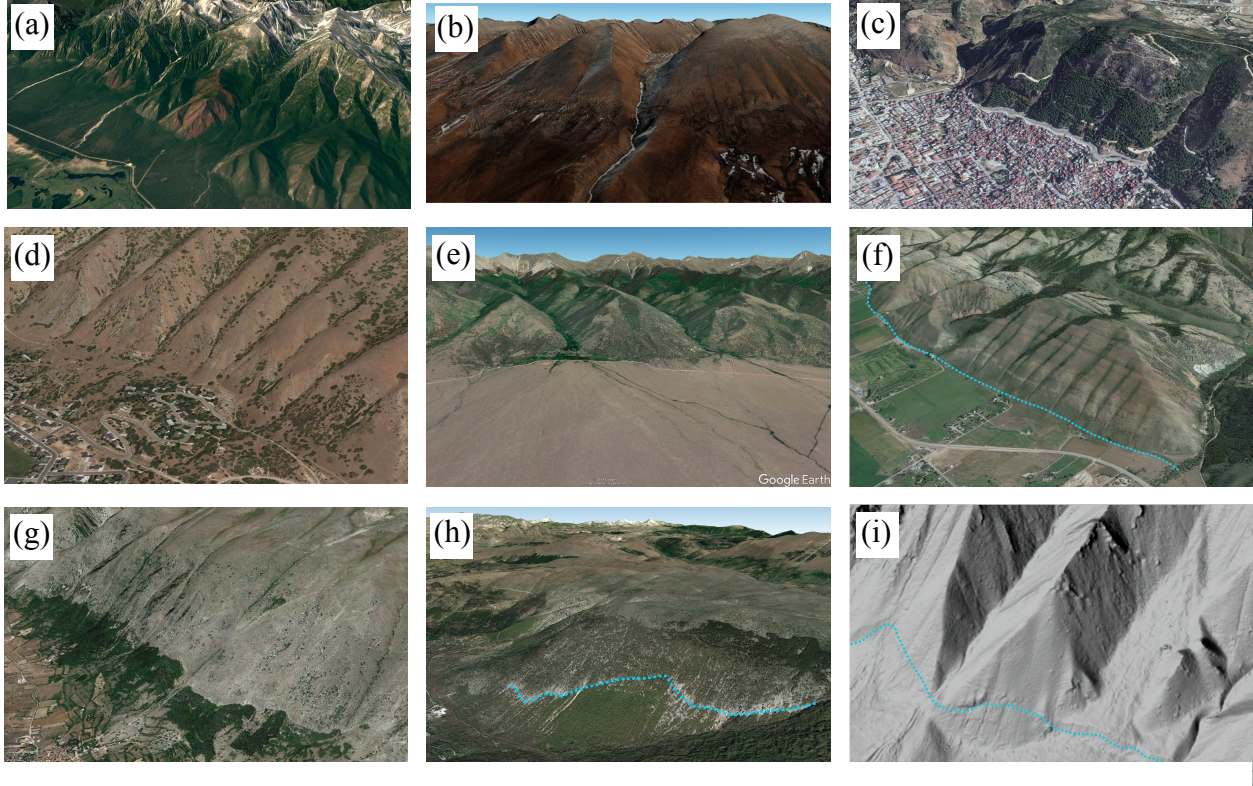
88 (o illustration with baselevel lowering)

89 - illustration with baselevel rise

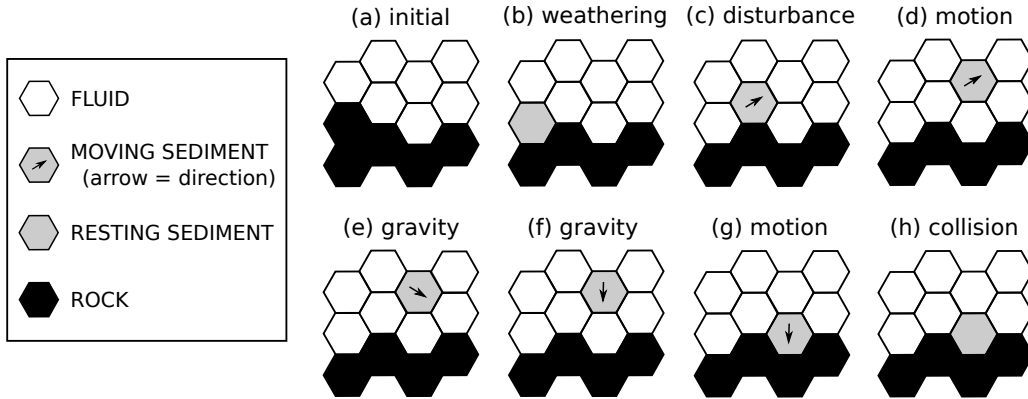
90 o illustration with time-varying w and/or d

$$\alpha - \theta = E/V \quad (1)$$

$$S' = \frac{2\delta s}{V} \quad (2)$$



91 **Figure 1.** Examples of normal-fault facets. (a) mountain front in Lake Baikal Rift Zone,  
 92 Russia. (b) Kung Co half graben, Tibet. (c) Hatay Graben, Antakya, Turkey [Boulton and Whit-  
 93 taker, 2009]. (d) Wasatch fault system, Provo section, near Springville, Utah, USA. (e) west  
 94 side of Sangre de Cristo range, San Luis Valley, Colorado, USA. (f) Star Valley fault, Wyoming,  
 95 USA. Note fault trace (light blue dotted line) at base of range front. (g) Magnola fault, central  
 96 Apennines, Italy. Vegetation break marks approximate location of fault trace. (h) Portion of the  
 97 Fucino fault near Gioi di Marsi, Italy. Fault trace shown in light blue dotted line. (i) Wasatch  
 98 fault system, Nephi section, Utah, USA. Fault trace shown in light blue dotted line.



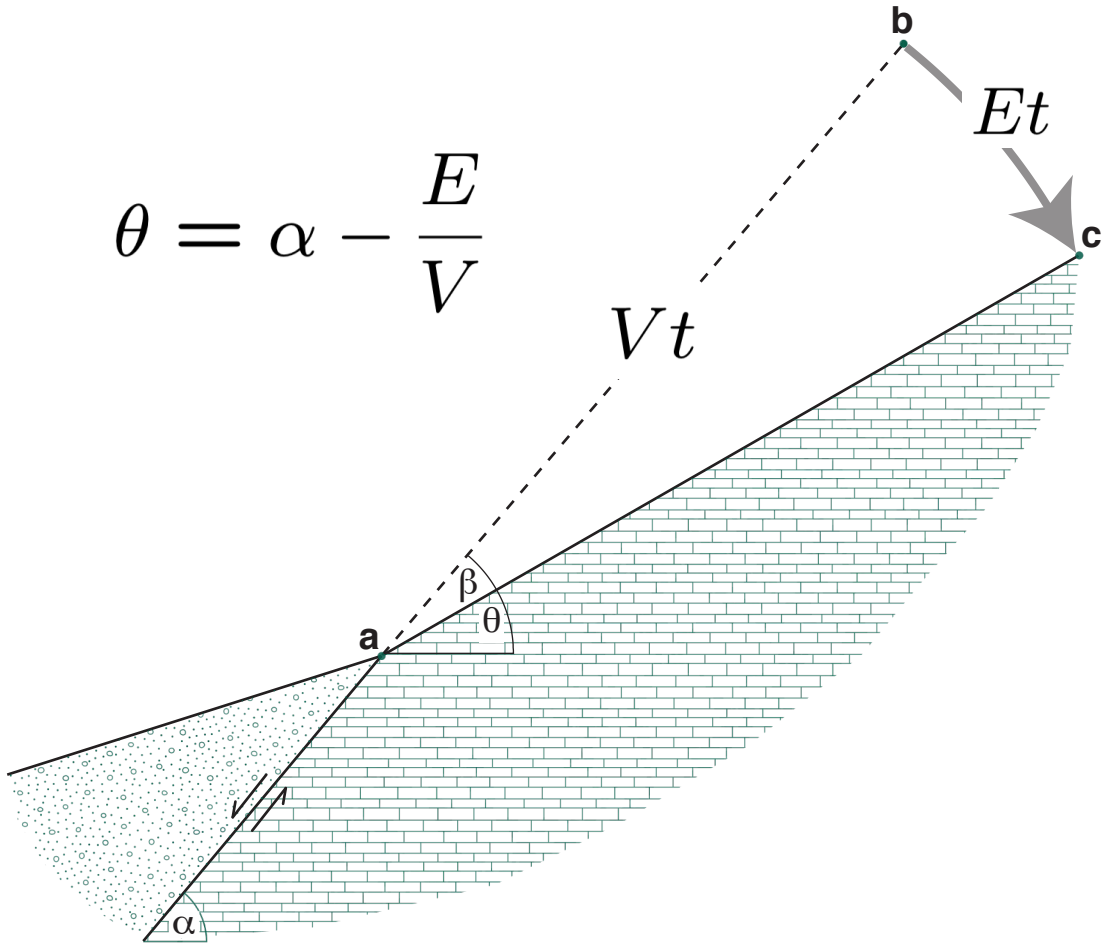
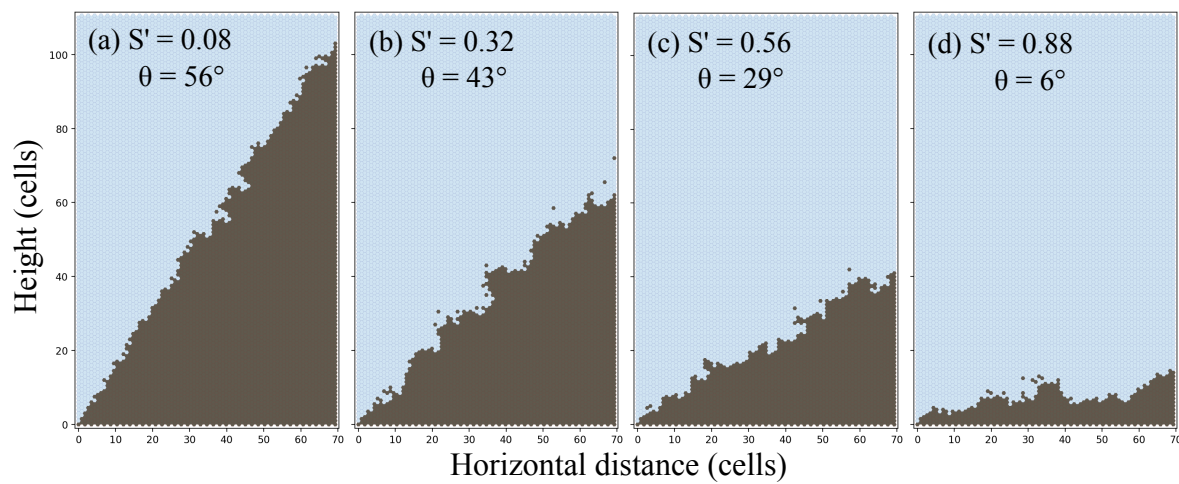
99      **Figure 2.** Illustration of cell states and pairwise transitions in the Grain Facet model. Each  
 100     cell assigned an integer from 0 to 8 that represents its state (0 is fluid, states 1–6 represent the  
 101     six directions of motion, state 7 is resting sediment, and state 8 is rock). (Figure modified from  
 102     Tucker et al. [2018]).

122    **Acknowledgments**

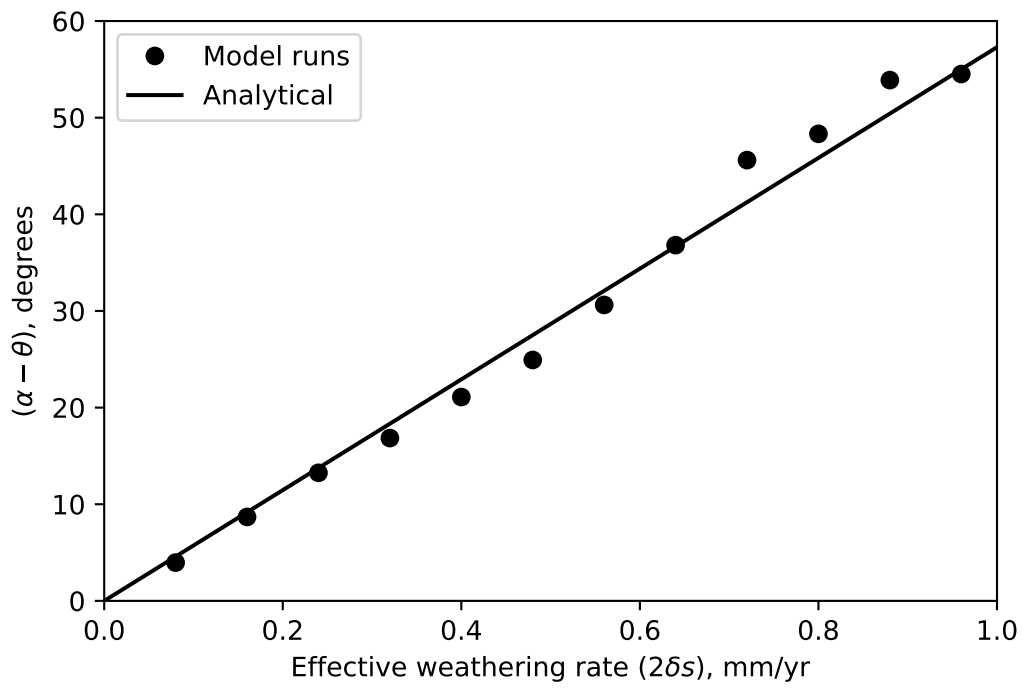
123    thanks

124    **References**

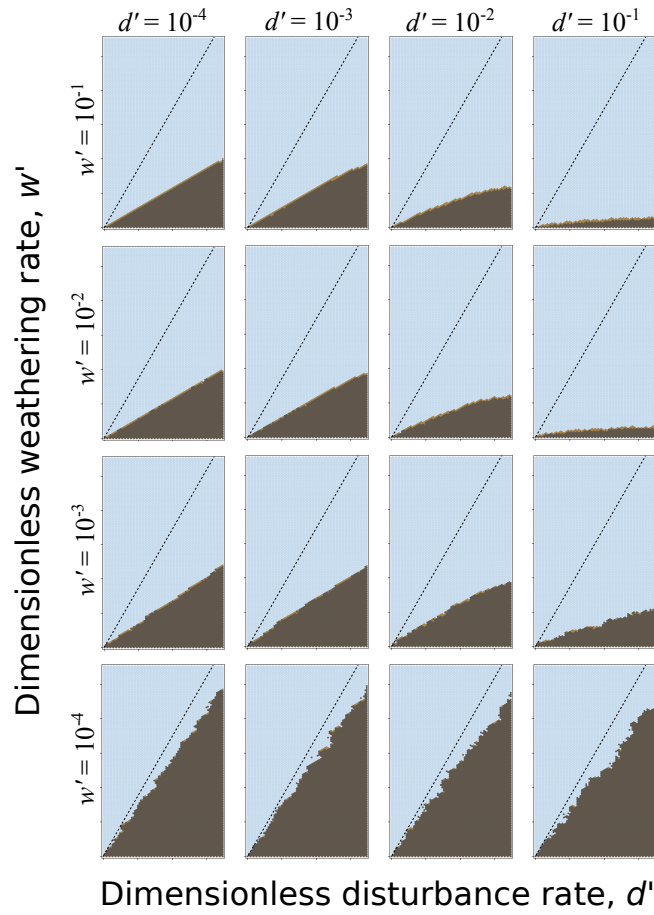
- 125    Boulton, S., and A. Whittaker (2009), Quantifying the slip rates, spatial distribution  
 126    and evolution of active normal faults from geomorphic analysis: Field examples  
 127    from an oblique-extensional graben, southern turkey, *Geomorphology*, 104 (3-4),  
 128    299–316.
- 129    Tucker, G. E., S. W. McCoy, and D. E. Hobley (2018), A lattice grain model of  
 130    hillslope evolution, *Earth Surface Dynamics*, 6(3), 563–582.

**Figure 3.**

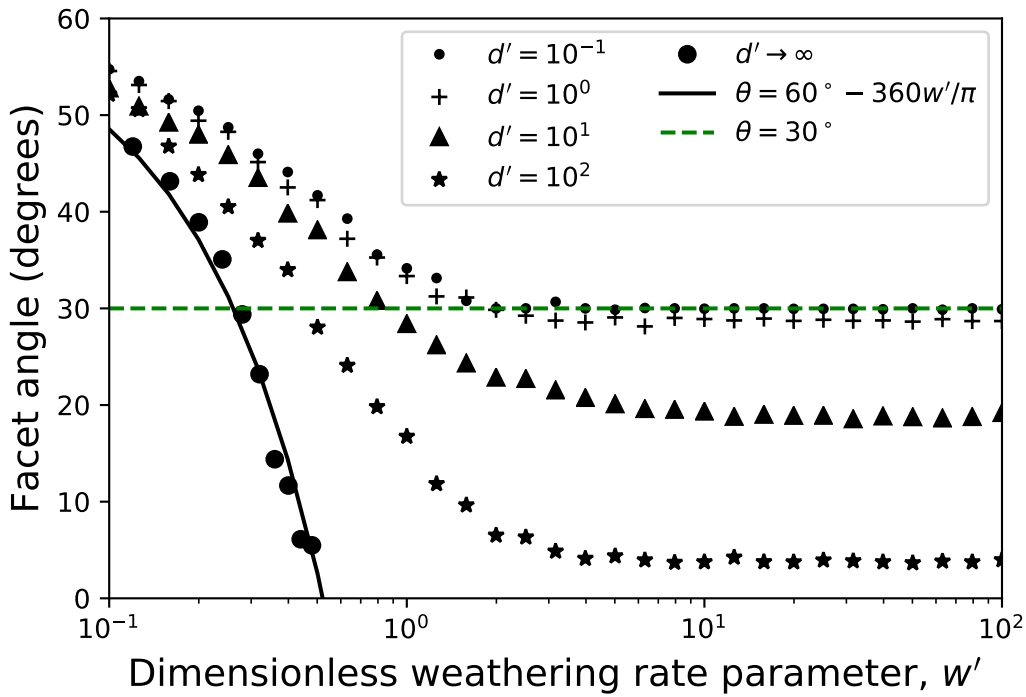
104      **Figure 4.** Simulated facet cross-sectional profiles formed under a combination of fault slip  
 105      and dissolution. Dark gray indicates rock, and light blue is air. Labels show the dimensionless  
 106      effective dissolution efficiency,  $S'$  (equation 2), and the average facet slope angle,  $\gamma$ .



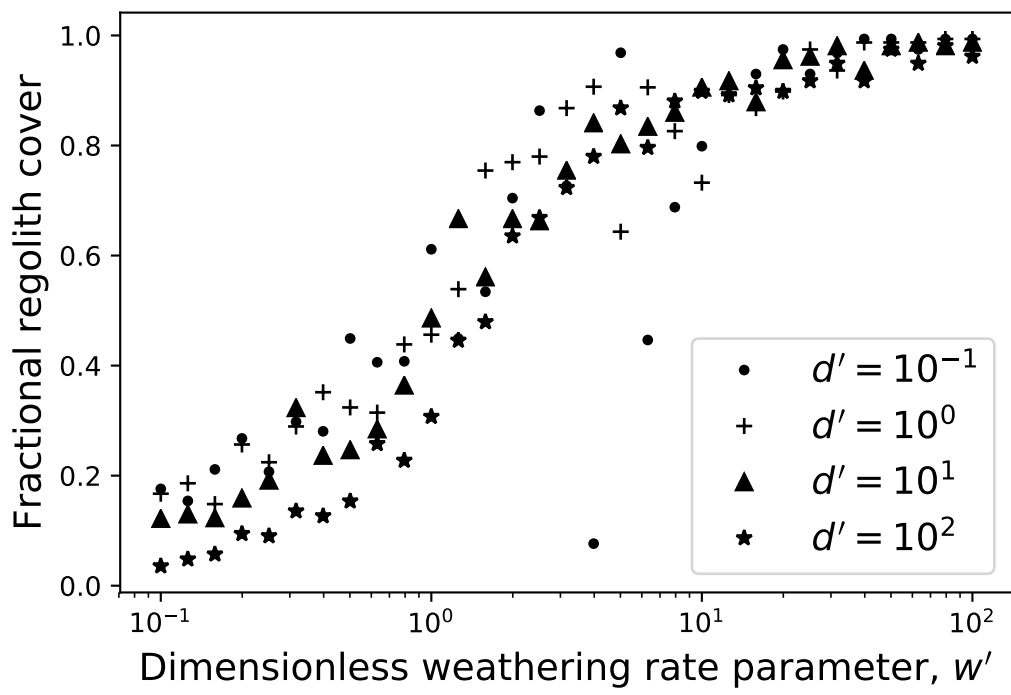
107      **Figure 5.** Difference in angle between fault plane ( $\alpha$ ) and facet ( $\gamma$ ), as a function of the  
108      nominal dissolution rate  $2\delta s$ , from runs with fault slip and dissolution (only). Solid circles show  
109      individual model runs, and line shows the prediction of equation 1.



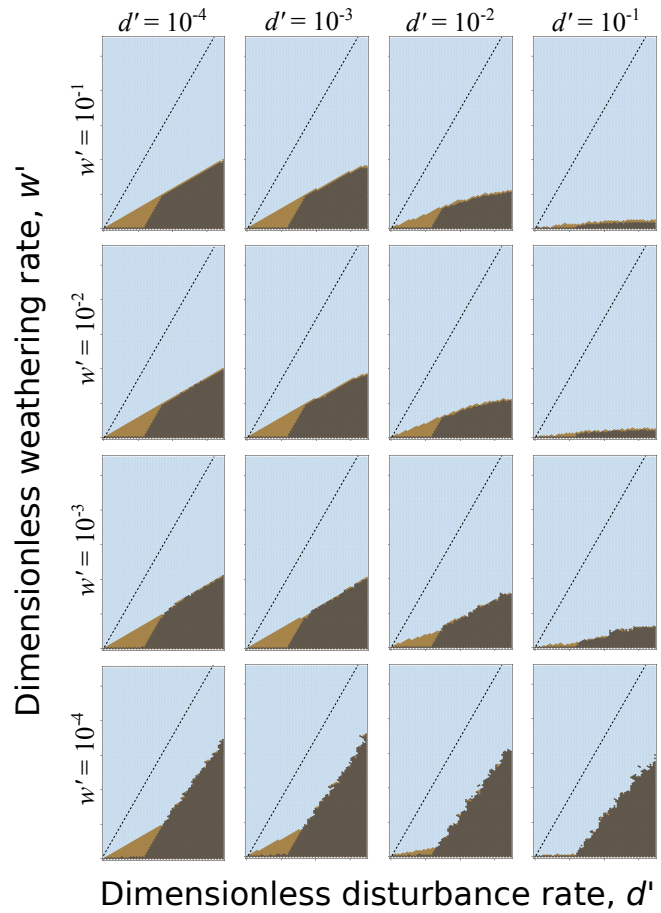
110 **Figure 6.** Examples of simulated facet profiles at varying values of  $d'$  and  $w'$ . Dotted line  
 111 shows projected fault plane.



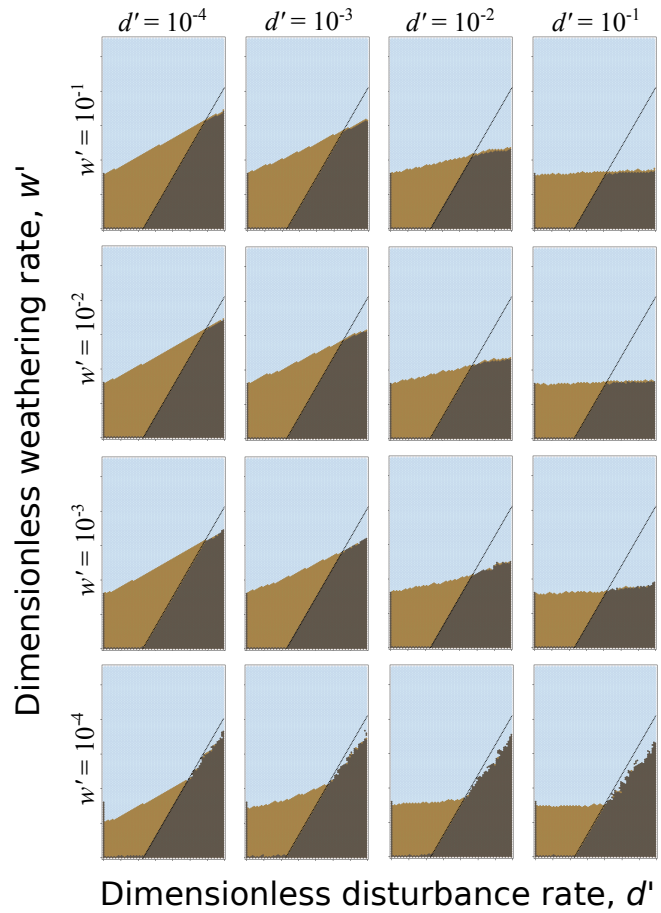
<sup>112</sup> **Figure 7.** Modeled equilibrium facet angle as a function of weathering and disturbance rate  
<sup>113</sup> parameters. Solid line shows the analytical solution for the case in which no regolith is produced  
<sup>114</sup> (all rock dissolves), which corresponds to an effectively infinite disturbance rate. Dashed line  
<sup>115</sup> shows the model's 30° effective angle of repose.



116 **Figure 8.** Modeled regolith cover proportion for steady facets, as a function of weathering and  
117 disturbance rate parameters. Scatter around the sigmoidal curve reflects stochastic variability.



118 **Figure 9.** Simulated facet profiles showing the development of a colluvial wedge on the hang-  
 119 ingwall.



120 **Figure 10.** Simulated facet profiles with a rising baselevel along the left model boundary,  
 121 representing an aggrading hangingwall basin.